Search for doubly charged Higgs boson pair production in ppbar collisions at sqrts = 1.96 TeV

V.M. Abazov, B. Abbott, B.S. Acharya, M. Adams, T. Adams, G.D. Alexeev, G. Alkhazov, A. Alton, G. Alverson, G.A. Alves, et al.

Fermilab-Pub-11/286-E

Search for doubly-charged Higgs boson pair production in $p\overline{p}$ collisions at $\sqrt{s} = 1.96$ TeV

V.M. Abazov,[35] B. Abbott,[73] B.S. Acharya,[29] M. Adams,[49] T. Adams,[47] G.D. Alexeev,[35] G. Alkhazov,[39] A. Alton[a],[61] G. Alverson,[60] G.A. Alves,[2] M. Aoki,[48] M. Arov,[58] A. Askew,[47] B. Åsman,[41] O. Atramentov,[65] C. Avila,[8] J. BackusMayes,[80] F. Badaud,[13] L. Bagby,[48] B. Baldin,[48] D.V. Bandurin,[47] S. Banerjee,[29] E. Barberis,[60] P. Baringer,[56] J. Barreto,[3] J.F. Bartlett,[48] U. Bassler,[18] V. Bazterra,[49] S. Beale,[6] A. Bean,[56] M. Begalli,[3] M. Begel,[71] C. Belanger-Champagne,[41] L. Bellantoni,[48] S.B. Beri,[27] G. Bernardi,[17] R. Bernhard,[22] I. Bertram,[42] M. Besançon,[18] R. Beuselinck,[43] V.A. Bezzubov,[38] P.C. Bhat,[48] V. Bhatnagar,[27] G. Blazey,[50] S. Blessing,[47] K. Bloom,[64] A. Boehnlein,[48] D. Boline,[70] E.E. Boos,[37] G. Borissov,[42] T. Bose,[59] A. Brandt,[76] O. Brandt,[23] R. Brock,[62] G. Brooijmans,[68] A. Bross,[48] D. Brown,[17] J. Brown,[17] X.B. Bu,[48] M. Buehler,[79] V. Buescher,[24] V. Bunichev,[37] S. Burdin[b],[42] T.H. Burnett,[80] C.P. Buszello,[41] B. Calpas,[15] E. Camacho-Pérez,[32] M.A. Carrasco-Lizarraga,[56] B.C.K. Casey,[48] H. Castilla-Valdez,[32] S. Chakrabarti,[70] D. Chakraborty,[50] K.M. Chan,[54] A. Chandra,[78] G. Chen,[56] S. Chevalier-Théry,[18] D.K. Cho,[75] S.W. Cho,[31] S. Choi,[31] B. Choudhary,[28] S. Cihangir,[48] D. Claes,[64] J. Clutter,[56] M. Cooke,[48] W.E. Cooper,[48] M. Corcoran,[78] F. Couderc,[18] M.-C. Cousinou,[15] A. Croc,[18] D. Cutts,[75] A. Das,[45] G. Davies,[43] K. De,[76] S.J. de Jong,[34] E. De La Cruz-Burelo,[32] F. Déliot,[18] M. Demarteau,[48] R. Demina,[69] D. Denisov,[48] S.P. Denisov,[38] S. Desai,[48] C. Deterre,[18] K. DeVaughan,[64] H.T. Diehl,[48] M. Diesburg,[48] P.F. Ding,[44] A. Dominguez,[64] T. Dorland,[80] A. Dubey,[28] L.V. Dudko,[37] D. Duggan,[65] A. Duperrin,[15] S. Dutt,[27] A. Dyshkant,[50] M. Eads,[64] D. Edmunds,[62] J. Ellison,[46] V.D. Elvira,[48] Y. Enari,[17] H. Evans,[52] A. Evdokimov,[71] V.N. Evdokimov,[38] G. Facini,[60] T. Ferbel,[69] F. Fiedler,[24] F. Filthaut,[34] W. Fisher,[62] H.E. Fisk,[48] M. Fortner,[50] H. Fox,[42] S. Fuess,[48] A. Garcia-Bellido,[69] V. Gavrilov,[36] P. Gay,[13] W. Geng,[15,62] D. Gerbaudo,[66] C.E. Gerber,[49] Y. Gershtein,[65] G. Ginther,[48,69] G. Golovanov,[35] A. Goussiou,[80] P.D. Grannis,[70] S. Greder,[19] H. Greenlee,[48] Z.D. Greenwood,[58] E.M. Gregores,[4] G. Grenier,[20] Ph. Gris,[13] J.-F. Grivaz,[16] A. Grohsjean,[18] S. Grünendahl,[48] M.W. Grünewald,[30] T. Guillemin,[16] F. Guo,[70] G. Gutierrez,[48] P. Gutierrez,[73] A. Haas[c],[68] S. Hagopian,[47] J. Haley,[60] L. Han,[7] K. Harder,[44] A. Harel,[69] J.M. Hauptman,[55] J. Hays,[43] T. Head,[44] T. Hebbeker,[21] D. Hedin,[50] H. Hegab,[74] A.P. Heinson,[46] U. Heintz,[75] C. Hensel,[23] I. Heredia-De La Cruz,[32] K. Herner,[61] G. Hesketh[d],[44] M.D. Hildreth,[54] R. Hirosky,[79] T. Hoang,[47] J.D. Hobbs,[70] B. Hoeneisen,[12] M. Hohlfeld,[24] Z. Hubacek,[10,18] N. Huske,[17] V. Hynek,[10] I. Iashvili,[67] Y. Ilchenko,[77] R. Illingworth,[48] A.S. Ito,[48] S. Jabeen,[75] M. Jaffré,[16] D. Jamin,[15] A. Jayasinghe,[73] R. Jesik,[43] K. Johns,[45] M. Johnson,[48] D. Johnston,[64] A. Jonckheere,[48] P. Jonsson,[43] J. Joshi,[27] A.W. Jung,[48] A. Juste,[40] K. Kaadze,[57] E. Kajfasz,[15] D. Karmanov,[37] P.A. Kasper,[48] I. Katsanos,[64] R. Kehoe,[77] S. Kermiche,[15] N. Khalatyan,[48] A. Khanov,[74] A. Kharchilava,[67] Y.N. Kharzheev,[35] M.H. Kirby,[51] J.M. Kohli,[27] A.V. Kozelov,[38] J. Kraus,[62] S. Kulikov,[38] A. Kumar,[67] A. Kupco,[11] T. Kurča,[20] V.A. Kuzmin,[37] J. Kvita,[9] S. Lammers,[52] G. Landsberg,[75] P. Lebrun,[20] H.S. Lee,[31] S.W. Lee,[55] W.M. Lee,[48] J. Lellouch,[17] L. Li,[46] Q.Z. Li,[48] S.M. Lietti,[5] J.K. Lim,[31] D. Lincoln,[48] J. Linnemann,[62] V.V. Lipaev,[38] R. Lipton,[48] Y. Liu,[7] Z. Liu,[6] A. Lobodenko,[39] M. Lokajicek,[11] R. Lopes de Sa,[70] H.J. Lubatti,[80] R. Luna-Garcia[e],[32] A.L. Lyon,[48] A.K.A. Maciel,[2] D. Mackin,[78] R. Madar,[18] R. Magaña-Villalba,[32] S. Malik,[64] V.L. Malyshev,[35] Y. Maravin,[57] J. Martínez-Ortega,[32] R. McCarthy,[70] C.L. McGivern,[56] M.M. Meijer,[34] A. Melnitchouk,[63] D. Menezes,[50] P.G. Mercadante,[4] M. Merkin,[37] A. Meyer,[21] J. Meyer,[23] F. Miconi,[19] N.K. Mondal,[29] G.S. Muanza,[15] M. Mulhearn,[79] E. Nagy,[15] M. Naimuddin,[28] M. Narain,[75] R. Nayyar,[28] H.A. Neal,[61] J.P. Negret,[8] P. Neustroev,[39] S.F. Novaes,[5] T. Nunnemann,[25] G. Obrant[‡],[39] J. Orduna,[78] N. Osman,[15] J. Osta,[54] G.J. Otero y Garzón,[1] M. Padilla,[46] A. Pal,[76] N. Parashar,[53] V. Parihar,[75] S.K. Park,[31] J. Parsons,[68] R. Partridge[c],[75] N. Parua,[52] A. Patwa,[71] B. Penning,[48] M. Perfilov,[37] K. Peters,[44] Y. Peters,[44] K. Petridis,[44] G. Petrillo,[69] P. Pétroff,[16] R. Piegaia,[1] M.-A. Pleier,[71] P.L.M. Podesta-Lerma[f],[32] V.M. Podstavkov,[48] P. Polozov,[36] A.V. Popov,[38] M. Prewitt,[78] D. Price,[52] N. Prokopenko,[38] S. Protopopescu,[71] J. Qian,[61] A. Quadt,[23] B. Quinn,[63] M.S. Rangel,[2] K. Ranjan,[28] P.N. Ratoff,[42] I. Razumov,[38] P. Renkel,[77] M. Rijssenbeek,[70] I. Ripp-Baudot,[19] F. Rizatdinova,[74] M. Rominsky,[48] A. Ross,[42] C. Royon,[18] P. Rubinov,[48] R. Ruchti,[54] G. Safronov,[36] G. Sajot,[14] P. Salcido,[50] A. Sánchez-Hernández,[32] M.P. Sanders,[25] B. Sanghi,[48] A.S. Santos,[5] G. Savage,[48] L. Sawyer,[58] T. Scanlon,[43] R.D. Schamberger,[70] Y. Scheglov,[39] H. Schellman,[51] T. Schliephake,[26] S. Schlobohm,[80] C. Schwanenberger,[44] R. Schwienhorst,[62] J. Sekaric,[56] H. Severini,[73] E. Shabalina,[23] V. Shary,[18] A.A. Shchukin,[38]

R.K. Shivpuri,[28] V. Simak,[10] V. Sirotenko,[48] P. Skubic,[73] P. Slattery,[69] D. Smirnov,[54] K.J. Smith,[67] G.R. Snow,[64] J. Snow,[72] S. Snyder,[71] S. Söldner-Rembold,[44] L. Sonnenschein,[21] K. Soustruznik,[9] J. Stark,[14] V. Stolin,[36] D.A. Stoyanova,[38] M. Strauss,[73] D. Strom,[49] L. Stutte,[48] L. Suter,[44] P. Svoisky,[73] M. Takahashi,[44] A. Tanasijczuk,[1] W. Taylor,[6] M. Titov,[18] V.V. Tokmenin,[35] Y.-T. Tsai,[69] D. Tsybychev,[70] B. Tuchming,[18] C. Tully,[66] L. Uvarov,[39] S. Uvarov,[39] S. Uzunyan,[50] R. Van Kooten,[52] W.M. van Leeuwen,[33] N. Varelas,[49] E.W. Varnes,[45] I.A. Vasilyev,[38] P. Verdier,[20] L.S. Vertogradov,[35] M. Verzocchi,[48] M. Vesterinen,[44] D. Vilanova,[18] P. Vokac,[10] H.D. Wahl,[47] M.H.L.S. Wang,[48] J. Warchol,[54] G. Watts,[80] M. Wayne,[54] M. Weber[g],[48] L. Welty-Rieger,[51] A. White,[76] D. Wicke,[26] M.R.J. Williams,[42] G.W. Wilson,[56] M. Wobisch,[58] D.R. Wood,[60] T.R. Wyatt,[44] Y. Xie,[48] C. Xu,[61] S. Yacoob,[51] R. Yamada,[48] W.-C. Yang,[44] T. Yasuda,[48] Y.A. Yatsunenko,[35] Z. Ye,[48] H. Yin,[48] K. Yip,[71] S.W. Youn,[48] J. Yu,[76] S. Zelitch,[79] T. Zhao,[80] B. Zhou,[61] J. Zhu,[61] M. Zielinski,[69] D. Zieminska,[52] and L. Zivkovic[75]

(The D0 Collaboration*)

[1]*Universidad de Buenos Aires, Buenos Aires, Argentina*
[2]*LAFEX, Centro Brasileiro de Pesquisas Físicas, Rio de Janeiro, Brazil*
[3]*Universidade do Estado do Rio de Janeiro, Rio de Janeiro, Brazil*
[4]*Universidade Federal do ABC, Santo André, Brazil*
[5]*Instituto de Física Teórica, Universidade Estadual Paulista, São Paulo, Brazil*
[6]*Simon Fraser University, Vancouver, British Columbia, and York University, Toronto, Ontario, Canada*
[7]*University of Science and Technology of China, Hefei, People's Republic of China*
[8]*Universidad de los Andes, Bogotá, Colombia*
[9]*Charles University, Faculty of Mathematics and Physics, Center for Particle Physics, Prague, Czech Republic*
[10]*Czech Technical University in Prague, Prague, Czech Republic*
[11]*Center for Particle Physics, Institute of Physics, Academy of Sciences of the Czech Republic, Prague, Czech Republic*
[12]*Universidad San Francisco de Quito, Quito, Ecuador*
[13]*LPC, Université Blaise Pascal, CNRS/IN2P3, Clermont, France*
[14]*LPSC, Université Joseph Fourier Grenoble 1, CNRS/IN2P3, Institut National Polytechnique de Grenoble, Grenoble, France*
[15]*CPPM, Aix-Marseille Université, CNRS/IN2P3, Marseille, France*
[16]*LAL, Université Paris-Sud, CNRS/IN2P3, Orsay, France*
[17]*LPNHE, Universités Paris VI and VII, CNRS/IN2P3, Paris, France*
[18]*CEA, Irfu, SPP, Saclay, France*
[19]*IPHC, Université de Strasbourg, CNRS/IN2P3, Strasbourg, France*
[20]*IPNL, Université Lyon 1, CNRS/IN2P3, Villeurbanne, France and Université de Lyon, Lyon, France*
[21]*III. Physikalisches Institut A, RWTH Aachen University, Aachen, Germany*
[22]*Physikalisches Institut, Universität Freiburg, Freiburg, Germany*
[23]*II. Physikalisches Institut, Georg-August-Universität Göttingen, Göttingen, Germany*
[24]*Institut für Physik, Universität Mainz, Mainz, Germany*
[25]*Ludwig-Maximilians-Universität München, München, Germany*
[26]*Fachbereich Physik, Bergische Universität Wuppertal, Wuppertal, Germany*
[27]*Panjab University, Chandigarh, India*
[28]*Delhi University, Delhi, India*
[29]*Tata Institute of Fundamental Research, Mumbai, India*
[30]*University College Dublin, Dublin, Ireland*
[31]*Korea Detector Laboratory, Korea University, Seoul, Korea*
[32]*CINVESTAV, Mexico City, Mexico*
[33]*Nikhef, Science Park, Amsterdam, the Netherlands*
[34]*Radboud University Nijmegen, Nijmegen, the Netherlands and Nikhef, Science Park, Amsterdam, the Netherlands*
[35]*Joint Institute for Nuclear Research, Dubna, Russia*
[36]*Institute for Theoretical and Experimental Physics, Moscow, Russia*
[37]*Moscow State University, Moscow, Russia*
[38]*Institute for High Energy Physics, Protvino, Russia*
[39]*Petersburg Nuclear Physics Institute, St. Petersburg, Russia*
[40]*Institució Catalana de Recerca i Estudis Avançats (ICREA) and Institut de Física d'Altes Energies (IFAE), Barcelona, Spain*
[41]*Stockholm University, Stockholm and Uppsala University, Uppsala, Sweden*
[42]*Lancaster University, Lancaster LA1 4YB, United Kingdom*
[43]*Imperial College London, London SW7 2AZ, United Kingdom*
[44]*The University of Manchester, Manchester M13 9PL, United Kingdom*
[45]*University of Arizona, Tucson, Arizona 85721, USA*
[46]*University of California Riverside, Riverside, California 92521, USA*
[47]*Florida State University, Tallahassee, Florida 32306, USA*

[48]Fermi National Accelerator Laboratory, Batavia, Illinois 60510, USA
[49]University of Illinois at Chicago, Chicago, Illinois 60607, USA
[50]Northern Illinois University, DeKalb, Illinois 60115, USA
[51]Northwestern University, Evanston, Illinois 60208, USA
[52]Indiana University, Bloomington, Indiana 47405, USA
[53]Purdue University Calumet, Hammond, Indiana 46323, USA
[54]University of Notre Dame, Notre Dame, Indiana 46556, USA
[55]Iowa State University, Ames, Iowa 50011, USA
[56]University of Kansas, Lawrence, Kansas 66045, USA
[57]Kansas State University, Manhattan, Kansas 66506, USA
[58]Louisiana Tech University, Ruston, Louisiana 71272, USA
[59]Boston University, Boston, Massachusetts 02215, USA
[60]Northeastern University, Boston, Massachusetts 02115, USA
[61]University of Michigan, Ann Arbor, Michigan 48109, USA
[62]Michigan State University, East Lansing, Michigan 48824, USA
[63]University of Mississippi, University, Mississippi 38677, USA
[64]University of Nebraska, Lincoln, Nebraska 68588, USA
[65]Rutgers University, Piscataway, New Jersey 08855, USA
[66]Princeton University, Princeton, New Jersey 08544, USA
[67]State University of New York, Buffalo, New York 14260, USA
[68]Columbia University, New York, New York 10027, USA
[69]University of Rochester, Rochester, New York 14627, USA
[70]State University of New York, Stony Brook, New York 11794, USA
[71]Brookhaven National Laboratory, Upton, New York 11973, USA
[72]Langston University, Langston, Oklahoma 73050, USA
[73]University of Oklahoma, Norman, Oklahoma 73019, USA
[74]Oklahoma State University, Stillwater, Oklahoma 74078, USA
[75]Brown University, Providence, Rhode Island 02912, USA
[76]University of Texas, Arlington, Texas 76019, USA
[77]Southern Methodist University, Dallas, Texas 75275, USA
[78]Rice University, Houston, Texas 77005, USA
[79]University of Virginia, Charlottesville, Virginia 22901, USA
[80]University of Washington, Seattle, Washington 98195, USA

(Dated: November 15, 2018)

We present a search for pair production of doubly-charged Higgs bosons in the processes $q\bar{q} \to H^{++}H^{--}$ decaying through $H^{\pm\pm} \to \tau^{\pm}\tau^{\pm}, \mu^{\pm}\tau^{\pm}, \mu^{\pm}\mu^{\pm}$. The search is performed in $p\overline{p}$ collisions at a center-of-mass energy of $\sqrt{s} = 1.96$ TeV using an integrated luminosity of up to 7.0 fb^{-1} collected by the D0 experiment at the Fermilab Tevatron Collider. The results are used to set 95% C.L. limits on the pair production cross section of doubly-charged Higgs bosons and on their mass for different $H^{\pm\pm}$ branching fractions. Models predicting different $H^{\pm\pm}$ decays are investigated. Assuming $\mathcal{B}(H^{\pm\pm} \to \tau^{\pm}\tau^{\pm}) = 1$ yields an observed (expected) lower limit on the mass of a left-handed $H_L^{\pm\pm}$ boson of 128 (116) GeV and assuming $\mathcal{B}(H^{\pm\pm} \to \mu^{\pm}\tau^{\pm}) = 1$ the corresponding limits are 144 (149) GeV. In a model with $\mathcal{B}(H^{\pm\pm} \to \tau^{\pm}\tau^{\pm}) = \mathcal{B}(H^{\pm\pm} \to \mu^{\pm}\tau^{\pm}) = \mathcal{B}(H^{\pm\pm} \to \mu^{\pm}\mu^{\pm}) = 1/3$, we obtain $M(H_L^{\pm\pm}) > 130$ (138) GeV.

PACS numbers: 14.80.Fd,13.85.Rm

Doubly-charged Higgs bosons ($H^{\pm\pm}$) appear in models with an extended Higgs sector such as the Little Higgs model [1], left-right symmetric models [2], and in models with $SU(3)_c \times SU(3)_L \times U(1)_Y$ (3-3-1) gauge symmetry [3].

The $H^{\pm\pm}$ bosons could be pair-produced and observed at a hadron collider through the process $q\bar{q} \to Z/\gamma^* \to H^{++}H^{--} \to \ell^+\ell'^+\ell^-\ell'^-$ ($\ell, \ell' = e, \mu, \tau$). Single production of $H^{\pm\pm}$ bosons through W exchange, leading to $H^{\pm\pm}H^{\mp}$ final states, is not considered in this Letter to reduce the model dependency of the results [4]. Some models favor a mass of the $H^{\pm\pm}$ boson at the electroweak scale [5]. The decay into like-charge lepton pairs violates lepton flavor number conservation. The decays $H^{\pm\pm} \to \tau^{\pm}\tau^{\pm}$ are predicted to dominate in some scenarios, such as the 3-3-1 model of Ref. [6]. In a Higgs triplet model that is based on a seesaw neutrino mass mechanism, a normal hierarchy of neutrino masses leads to approximately equal branching fractions for $H^{\pm\pm}$ boson

*with visitors from [a]Augustana College, Sioux Falls, SD, USA, [b]The University of Liverpool, Liverpool, UK, [c]SLAC, Menlo Park, CA, USA, [d]University College London, London, UK, [e]Centro de Investigacion en Computacion - IPN, Mexico City, Mexico, [f]ECFM, Universidad Autonoma de Sinaloa, Culiacán, Mexico, and [g]Universität Bern, Bern, Switzerland. [‡]Deceased.

decays to $\tau\tau$, $\mu\tau$, and $\mu\mu$, if the mass of the lightest neutrino is less than 10 meV [7]. In this Letter, we present the first comparison of data with this model and the first search for $H^{\pm\pm} \to \tau^{\pm}\tau^{\pm}$ decays at a hadron collider.

In left-right symmetric models, right-handed states ($H_R^{\pm\pm}$) appear in addition to left-handed states ($H_L^{\pm\pm}$). They are characterized through their coupling to right-handed and left-handed fermions, respectively. The cross section for production of right-handed $H_R^{++}H_R^{--}$ pairs is about a factor of 2 smaller than for $H_L^{++}H_L^{--}$ because of the different coupling to the Z boson [8]. The mass limits for $H_R^{\pm\pm}$ bosons therefore tend to be weaker than for $H_L^{\pm\pm}$ bosons.

Searches for production of $H^{\pm\pm}$ bosons have been performed previously at the CERN e^+e^- Collider (LEP) [9] and at the DESY ep Collider (HERA) [10]. Limits on the mass of the $H^{\pm\pm}$ boson were obtained in the range of $95-100$ GeV, depending on the flavor of the final state leptons. The OPAL and H1 Collaborations searched for single $H^{\pm\pm}$ production in the processes $e^+e^- \to e^{\mp}e^{\mp}H^{\pm\pm}$ [11] and $e^{\pm}p \to \ell^{\mp}H^{\pm\pm}p$ [10], and through the study of Bhabha scattering $e^+e^- \to e^+e^-$ [11], constraining the $H^{\pm\pm}$ boson's Yukawa couplings h_{ee} to electrons. Bounds on decays such as $\tau \to 3\mu$ or $\mu \to e\gamma$ and the measured $(g-2)_\mu$ also constrain different $h_{\ell\ell'}$ [12]. At the Fermilab Tevatron Collider, the D0 and CDF Collaborations published limits for $\mu\mu$, ee, $e\tau$, and $\mu\tau$ final states in the range $M(H_L^{\pm\pm}) > 112-150$ GeV, assuming 100% decays into the specified final state [13–16].

The results in this Letter are based on data collected with the D0 detector at the Fermilab Tevatron Collider and correspond to an integrated luminosity of up to 7.0 fb^{-1}. The D0 detector [17] comprises tracking detectors and calorimeters. Silicon microstrip detectors and a scintillating fiber tracker are used to reconstruct charged particle tracks within a 2 T solenoid. The uranium and liquid-argon calorimeters used to measure particle energies consist of electromagnetic (EM) and hadronic sections. Muons are identified by combining tracks in the central tracker with patterns of hits in the muon spectrometer. Events are required to pass triggers that select at least one muon candidate.

All background processes are simulated using Monte Carlo (MC) event generators, except the multijet background, which is determined from data. The W+jet, $Z/\gamma^* \to \ell^+\ell^-$, and $t\bar{t}$ processes are generated using ALPGEN [18] with showering and hadronization provided by PYTHIA [19]. Diboson production (WW, WZ, and ZZ) and signal events are simulated using PYTHIA. The signal samples for the model with equal branching ratios for the decays $H^{\pm\pm} \to \tau^{\pm}\tau^{\pm}$, $\mu^{\pm}\mu^{\pm}$, and $\mu^{\pm}\tau^{\pm}$ are generated using Yukawa couplings $h_{\mu\tau} = h_{\tau\mu} = \sqrt{2}h_{\tau\tau} = \sqrt{2}h_{\mu\mu}$. The tau lepton decays are simulated with TAUOLA [20], which includes a full treatment of the tau polarization. All MC samples are processed through a GEANT [21] simulation of the detector. Data from random beam crossings are overlaid on MC events to account for detector noise and additional $p\overline{p}$ interactions. The simulated distributions are corrected for the dependence of the trigger efficiency in data on the instantaneous luminosity and for differences between data and simulation in the reconstruction efficiencies and in the distribution of the longitudinal coordinate of the interaction point along the beam direction. Next-to-leading order (NLO) quantum chromodynamics calculations of cross sections are used to normalize the signal and the background contribution of diboson processes, and next-to-NLO calculations are used for all other processes.

Two types of tau lepton decays into hadrons (τ_h) are identified by their signatures: Type-1 tau candidates consist of a calorimeter cluster, with one associated track and no subcluster in the EM section of the calorimeter. This signature corresponds mainly to $\tau^{\pm} \to \pi^{\pm}\nu$ decays. For type-2 tau candidates, an energy deposit in the EM calorimeter is required in addition to the type-1 signature, as expected for $\tau^{\pm} \to \pi^{\pm}\pi^0\nu$ decays. The outputs of neural networks, one for each tau-type, designed to discriminate τ_h from jets, have to be $NN_\tau > 0.75$ [22]. Their input variables are based on isolation variables for objects and on the spatial distribution of showers. The tau lepton energy is measured with the calorimeter.

We select events with at least one muon and at least two τ_h candidates. The muons must be isolated, both in the tracking detectors and in the calorimeters. Each event must have a reconstructed $p\overline{p}$ interaction vertex with a longitudinal component located within 60 cm of the nominal center of the detector. The longitudinal coordinate $z_{\rm dca}$ of the distance of closest approach for each track is measured with respect to the nominal center of the detector. The differences between $z_{\rm dca}$ of the highest-p_T muon and the two highest-p_T τ_h (labeled τ_1 and τ_2), must be less than 2 cm. The pseudorapidity [23] of the selected muons, τ_1, and τ_2 must be $|\eta^\mu| < 1.6$ and $|\eta^{\tau_{1,2}}| < 1.5$, respectively, and for additional τ_h candidates we require $|\eta^\tau| < 2$. The transverse momenta must be $p_T^\mu > 15$ GeV and $p_T^{\tau_{1,2}} > 12.5$ GeV. All selected τ_h candidates and muons are required to be separated by $\Delta\mathcal{R}_{\mu\tau} > 0.5$, where $\Delta\mathcal{R} = \sqrt{(\Delta\phi)^2 + (\Delta\eta)^2}$ and ϕ is the azimuthal angle, and the two leading τ_h must be separated by $\Delta\mathcal{R}_{\tau_1\tau_2} > 0.7$. The sum of the charges of the highest-p_T muon, τ_1, and τ_2 is required to be $Q = \sum_{i=\mu,\tau_1,\tau_2} q_i = \pm 1$ as expected for signal. After all selections, the main background is from diboson production and $Z \to \tau^+\tau^-$, where an additional jet mimics a lepton.

We estimate the multijet background using three independent data samples and identical selections, except with the NN_τ requirements reversed, by requiring that either one or both τ_h candidates have $NN_\tau < 0.75$. The simulated background is subtracted before the samples are used to determine the differential distributions and normalization of the multijet background in the signal

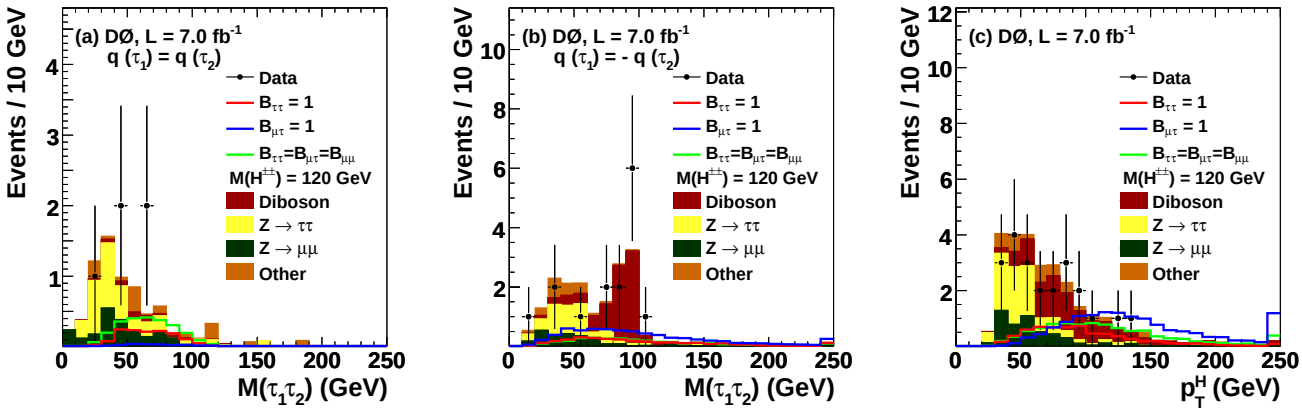

FIG. 1: (color online). $M(\tau_1,\tau_2)$ distribution for the (a) $q_{\tau_1} = q_{\tau_2}$ and (b) $q_{\tau_1} = -q_{\tau_2}$ samples, and (c) transverse momentum of the doubly-charged dilepton system p_T^H, for all four samples combined, after all selections. The data are compared to the sum of the expected background and to simulations of a $H_L^{\pm\pm}H_L^{\pm\pm}$ signal for $M(H^{\pm\pm}) = 120$ GeV and $\mathcal{B}(H_L^{\pm\pm} \to \tau^\pm\tau^\pm) = 1$, $\mathcal{B}(H_L^{\pm\pm} \to \mu^\pm\tau^\pm) = 1$, and $\mathcal{B}(H_L^{\pm\pm} \to \tau^\pm\tau^\pm) = \mathcal{B}(H_L^{\pm\pm} \to \mu^\pm\mu^\pm) = \mathcal{B}(H_L^{\pm\pm} \to \mu^\pm\tau^\pm) = 1/3$, normalized using the NLO calculation of the cross section. "Other" background comprises W+jet, $Z/\gamma^* \to e^+e^-$, and $t\bar{t}$ processes. All entries exceeding the range of the histogram are added to the last bin.

TABLE I: Numbers of events in data, predicted background, and expected signal for $M(H_L^{\pm\pm}) = 120$ GeV, assuming the NLO calculation of the signal cross section for $\mathcal{B}(H_L^{\pm\pm} \to \tau^\pm\tau^\pm) = 1$, $\mathcal{B}(H_L^{\pm\pm} \to \mu^\pm\tau^\pm) = 1$, and $\mathcal{B}(H_L^{\pm\pm} \to \tau^\pm\tau^\pm) = \mathcal{B}(H_L^{\pm\pm} \to \mu^\pm\mu^\pm) = \mathcal{B}(H_L^{\pm\pm} \to \mu^\pm\tau^\pm) = 1/3$. The numbers are shown for the four samples separately, together with their total uncertainties.

	All	$N_\mu = 1$ $N_\tau = 2$		$N_\mu = 1$ $N_\tau = 3$	$N_\mu = 2$ $N_\tau = 2$
		$q_{\tau_1} = q_{\tau_2}$	$q_{\tau_1} = -q_{\tau_2}$		
Signal					
$\tau^\pm\tau^\pm$	6.6 ± 0.9	1.4 ± 0.2	3.1 ± 0.4	1.6 ± 0.2	0.4 ± 0.1
$\mu^\pm\tau^\pm$	13.9 ± 1.9	0.3 ± 0.1	6.8 ± 0.9	0.4 ± 0.1	6.3 ± 0.9
Equal $\mathcal{B}$	9.5 ± 1.3	2.5 ± 0.3	3.1 ± 1.0	1.2 ± 0.2	2.6 ± 0.4
Background					
$Z \to \tau^+\tau^-$	8.2 ± 1.1	3.4 ± 0.5	4.8 ± 0.7	< 0.1	< 0.1
$Z \to \mu^+\mu^-$	5.1 ± 0.7	2.2 ± 0.3	2.5 ± 0.4	0.1 ± 0.1	0.2 ± 0.1
$Z \to e^+e^-$	0.3 ± 0.1	< 0.1	0.3 ± 0.1	< 0.1	< 0.1
W + jets	2.9 ± 0.4	1.1 ± 0.2	1.8 ± 0.3	< 0.1	< 0.1
$t\bar{t}$	0.6 ± 0.1	0.3 ± 0.1	0.3 ± 0.1	0.1 ± 0.1	< 0.1
Diboson	10.5 ± 1.7	0.5 ± 0.1	8.5 ± 1.4	0.4 ± 0.1	1.1 ± 0.2
Multijet	< 0.8	< 0.2	< 0.5	< 0.1	< 0.1
Background Sum	27.6 ± 4.9	7.5 ± 1.2	18.2 ± 3.3	0.6 ± 0.1	1.3 ± 0.2
Data	22	5	15	0	2

region. A second method used to estimate the multijet background is based on the fact that events with $Q = \pm 1$ are signal-like, whereas events with $Q = \pm 3$ correspond largely to multijet background. To reduce the W+jets contribution in the sample with $Q = \pm 3$, the visible W boson mass $M_W = \sqrt{2p^\mu \not{p}_T(1 - \cos\phi)}$ is required to be < 50 GeV, where p^μ is the muon momentum, $\not{p}_T$ the imbalance in transverse momentum measured in the calorimeter, and ϕ is the azimuthal angle between the muon and the direction of the $\not{p}_T$. The total rate of expected multijet background events following all selections is negligible ($< 3\%$ of the total background). We also use the sample where both τ_h candidates have $NN_\tau < 0.75$ to study the rate of jets that are falsely reconstructed as τ_h and we find this rate to be well modeled by the simulation.

To improve the discrimination of signal from background, the data are subdivided into four nonoverlapping samples, depending on the charges of the muon (q_μ) and the τ_h candidates (q_τ) and the number of muons (N_μ) and τ_h (N_τ) in the event. First, we define two samples for events with $N_\mu = 1$ and $N_\tau = 2$. Because the two like-charge leptons are assumed to originate from a single $H^{\pm\pm}$ decay, we consider separately events where both tau leptons have the same charge, $q_{\tau_1} = q_{\tau_2}$, and events with τ_1 and τ_2 of opposite charge, i.e., $q_{\tau_1} = -q_{\tau_2}$, which implies that one of the τ leptons and the muon have the same charge. The third sample is defined by $N_\tau = 3$ and the fourth sample by $N_\mu = 2$, without any additional requirements on the charges.

The distributions of the invariant mass of the two leading tau candidates, $M(\tau_1,\tau_2)$, for the like and opposite-charge samples are shown in Figs. 1(a) and (b). The separation into samples with different fractions of signal and background events increases the sensitivity to signal, as the composition of the background is different, with the like-charge sample being dominated by background from Z+jets decays and the opposite-charge sample by background from diboson production. The diboson background is mainly due to $WZ \to \mu\nu e^+e^-$ events where the electrons are misidentified as tau leptons. In Fig. 1(c) we show the transverse momentum of the doubly-charged dilepton system, p_T^H, which corresponds to the reconstructed $H^{\pm\pm} \to \ell^\pm\ell'^\pm$ decay, where $\ell^\pm\ell'^\pm = (\mu^\pm\tau_1^\pm, \mu^\pm\tau_2^\pm, \tau_1^\pm\tau_2^\pm)$ is the pairing of the two

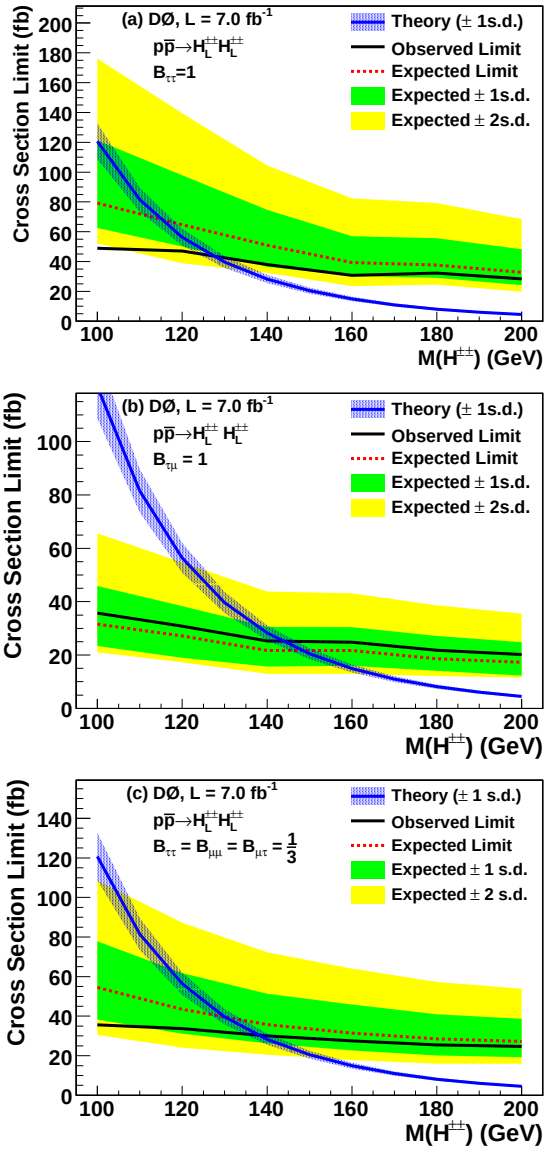

FIG. 2: (color online). Upper limit on the $H_L^{\pm\pm}H_L^{\pm\pm}$ pair production cross section for (a) $\mathcal{B}(H_L^{\pm\pm} \to \tau^\pm\tau^\pm) = 1$, (b) $\mathcal{B}(H_L^{\pm\pm} \to \mu^\pm\tau^\pm) = 1$, and (c) $\mathcal{B}(H_L^{\pm\pm} \to \tau^\pm\tau^\pm) = \mathcal{B}(H_L^{\pm\pm} \to \mu^\pm\mu^\pm) = \mathcal{B}(H_L^{\pm\pm} \to \mu^\pm\tau^\pm) = 1/3$. The bands around the median expected limits correspond to regions of ±1 and ±2 standard deviation (s.d.), and the band around the predicted NLO cross section for signal corresponds to a theoretical uncertainty of $\pm10\%$.

highest-p_T τ_h and the highest-p_T muon that have the same charges. Since $|Q| = 1$, only one such pairing exists per event. The expected number of background and signal events for the four samples and the observed numbers of events in data are shown in Table I with the statistical uncertainties of the MC samples and systematic uncertainties added in quadrature.

Since the data are well described by the background expectation, we determine limits on the $H^{++}H^{--}$ production cross section using a modified frequentist approach [24]. A log-likelihood ratio (LLR) test statistic is formed using the Poisson probabilities for estimated background yields, the signal acceptance, and the observed number of events for different $H^{\pm\pm}$ mass hypotheses. The confidence levels are derived by integrating the LLR distribution in pseudoexperiments using both the signal-plus-background (CL_{s+b}) and the background-only hypotheses (CL_b). The excluded production cross section is taken to be the cross section for which the confidence level for signal, $CL_s = CL_{s+b}/CL_b$, equals 0.05. The $M(\tau_1, \tau_2)$ distribution is used to discriminate signal from background.

TABLE II: Expected and observed limits on $M(H^{\pm\pm})$ (in GeV) for left-handed and right-handed $H^{\pm\pm}$ bosons. Only left-handed states exist in the model that assumes equality of branching fractions into $\tau\tau$, $\mu\tau$, and $\mu\mu$ final states. We only derive limits if the expected limit on $M(H^{\pm\pm})$ is ≥ 90 GeV.

Decay	$H_L^{\pm\pm}$		$H_R^{\pm\pm}$	
	expected	observed	expected	observed
$\mathcal{B}(H^{\pm\pm} \to \tau^\pm\tau^\pm) = 1$	116	128		
$\mathcal{B}(H^{\pm\pm} \to \mu^\pm\tau^\pm) = 1$	149	144	119	113
Equal $\mathcal{B}$ into $\tau^\pm\tau^\pm, \mu^\pm\mu^\pm, \mu^\pm\tau^\pm$	130	138		
$\mathcal{B}(H^{\pm\pm} \to \mu^\pm\mu^\pm) = 1$	180	168	154	145

In Fig. 2, the upper limits on the cross sections are compared to the NLO signal cross sections for $H_L^{\pm\pm}H_L^{\pm\pm}$ pair production [8] for some of the branching ratios considered. The corresponding expected and observed limits are shown in Table II.

The $H^{\pm\pm}$ boson mass limits assuming $\mathcal{B}(H^{\pm\pm} \to \tau^\pm\tau^\pm) + \mathcal{B}(H^{\pm\pm} \to \mu^\pm\mu^\pm) = 1$ are determined by combining signal samples generated with pure 4τ, $(2\tau/2\mu)$, and 4μ final states with fractions $\mathcal{B}^2$, $2\mathcal{B}(1-\mathcal{B})$, and $(1-\mathcal{B})^2$, respectively, where $\mathcal{B} \equiv \mathcal{B}(H^{\pm\pm} \to \tau^\pm\tau^\pm)$. Here, we include in the limit setting the distribution of the invariant mass of the two highest p_T muons, including the systematic uncertainties and their correlations, from a search for $H^{++}H^{--} \to 4\mu$ decays performed by

Systematic uncertainties on both background and signal, including their correlations, are taken into account. The theoretical uncertainty on background cross sections for $Z/\gamma^* \to \ell^+\ell^-$, W+jets, $t\bar{t}$, and dibo son production vary between $6\% - 10\%$. The uncertainty on the measured integrated luminosity is 6.1% [25]. The systematic uncertainty on muon identification is 2.9% per muon and the uncertainty on the identification of τ_h, including the uncertainty from applying a neural network to discriminate τ_h from jets, is 4% for each type-1 and 7% for each type-2 τ_h candidate. The trigger efficiency has a systematic uncertainty of 5%. The uncertainty on the signal acceptance from parton distribution functions is 4%.

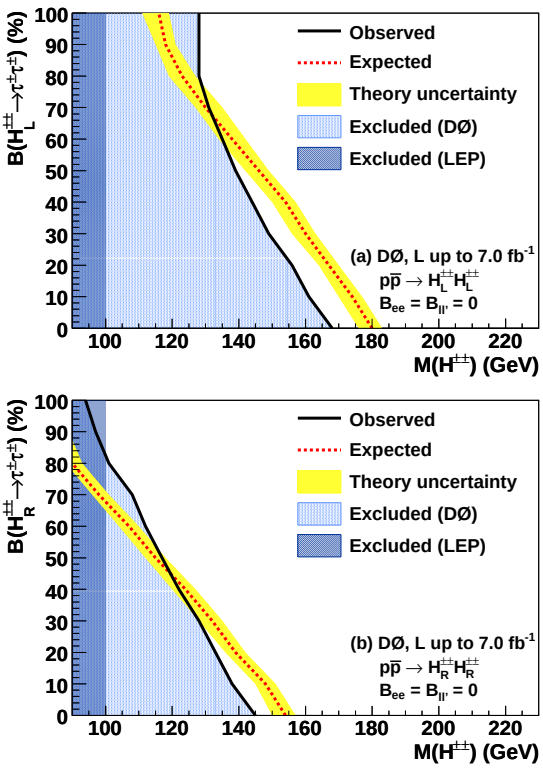

FIG. 3: (color online). Expected and observed exclusion region at the 95% C.L. in the plane of $\mathcal{B}(H^{\pm\pm} \to \tau^{\pm}\tau^{\pm})$ versus $M(H^{\pm\pm})$, assuming $\mathcal{B}(H^{\pm\pm} \to \tau^{\pm}\tau^{\pm}) + \mathcal{B}(H^{\pm\pm} \to \mu^{\pm}\mu^{\pm}) = 1$, for (a) left-handed and (b) right-handed $H^{\pm\pm}$ bosons. The band around the expected limit represents the uncertainty on the NLO calculation of the cross section for signal.

the D0 Collaboration in 1.1 fb^{-1} of integrated luminosity [13]. The results are shown in Fig. 3 for varying $\mathcal{B} = 0\% - 100\%$ in steps of 10%. When performing this analysis, we found that the statistical uncertainties on the background simulations were overestimated in [13]. A standard treatment of the uncertainties in the limit setting improves the mass limits for the 4μ final state, as shown in Table II.

In summary, we have performed the first search at a hadron collider for pair production of doubly-charged Higgs bosons decaying exclusively into tau leptons. We set an observed (expected) lower limit of $M(H_L^{\pm\pm}) > 128$ (116) GeV for a 100% branching fraction of $H^{\pm\pm} \to \tau^{\pm}\tau^{\pm}$, $M(H_L^{\pm\pm}) > 144$ (149) GeV for a 100% branching fraction into $\mu\tau$, and $M(H_L^{\pm\pm}) > 130$ (138) GeV for a model with equal branching ratios into $\tau\tau$, $\mu\tau$, and $\mu\mu$. These are the most stringent limits on $H^{\pm\pm}$ boson masses in these decay channels.

We thank the staffs at Fermilab and collaborating institutions, and acknowledge support from the DOE and NSF (USA); CEA and CNRS/IN2P3 (France); FASI, Rosatom and RFBR (Russia); CNPq, FAPERJ, FAPESP and FUNDUNESP (Brazil); DAE and DST (India); Colciencias (Colombia); CONACyT (Mexico); KRF and KOSEF (Korea); CONICET and UBACyT (Argentina); FOM (The Netherlands); STFC and the Royal Society (United Kingdom); MSMT and GACR (Czech Republic); CRC Program and NSERC (Canada); BMBF and DFG (Germany); SFI (Ireland); The Swedish Research Council (Sweden); and CAS and CNSF (China).

[1] N. Arkani-Hamed *et al.*, J. High Energy Phys. **08**, 021 (2002).
[2] R.N. Mohapatra and G. Senjanovic, Phys. Rev. Lett. 44, 912 (1980); R.N. Mohapatra and G. Senjanovic, Phys. Rev. **D 23**, 165 (1981); J.F. Gunion *et al.*, Phys. Rev. D **40**, 1546 (1989); N.G. Deshpande *et al.*, Phys. Rev. D **44**, 837 (1991).
[3] J.E. Cieza Montalvo *et al.*, Nucl. Phys. **B756**, 1 (2006); erratum-ibid. **B796**, 422 (2008).
[4] A.G. Akeroyd and M. Aoki, Phys. Rev. D **72**, 035011 (2005).
[5] C.S. Aulakh, A. Melfo, and G. Senjanovic, Phys. Rev. D **57**, 4174 (1998); Z. Chacko and R. N. Mohapatra, Phys. Rev. D **58**, 015003 (1998).
[6] E. Ramirez Barreto, Y.A. Coutinho, and J. Sá Borges, Phys. Rev. D **83**, 075001 (2011).
[7] M. Kadastik, M. Raidal, and L. Rebane, Phys. Rev. D **77**, 115023 (2008); A. Hektor *et al.*, Nucl. Phys. **B787**, 198 (2007).
[8] M. Mühlleitner and M. Spira, Phys. Rev. D **68**, 117701 (2003) and private communications.
[9] G. Abbiendi *et al.* (OPAL Collaboration), Phys. Lett. B **526**, 221 (2002); P. Achard *et al.* (L3 Collaboration), Phys. Lett. B **576**, 18 (2003); J. Abdallah *et al.* (DELPHI Collaboration), Phys. Lett. B **552**, 127 (2003).
[10] A. Aktas *et al.* (H1 Collaboration), Phys. Lett. B **638**, 432 (2006).
[11] G. Abbiendi *et al.* (OPAL Collaboration), Phys. Lett. B **577**, 93 (2003).
[12] J.F. Gunion *et al.*, Phys. Rev. D **40**, 1546 (1989); R.N. Mohapatra, Phys. Rev. D **46**, 2990 (1992).
[13] V.M. Abazov *et al.* (D0 Collaboration), Phys. Rev. Lett. **101**, 071803 (2008).
[14] V.M. Abazov *et al.* (D0 Collaboration), Phys. Rev. Lett. **93** 141801 (2004).
[15] D. Acosta *et al.* (CDF Collaboration), Phys. Rev. Lett. **93**, 221802 (2004).
[16] T. Aaltonen *et al.* (CDF Collaboration), Phys. Rev. Lett. **101**, 121801 (2008).
[17] V.M. Abazov *et al.* (D0 Collaboration), Nucl. Instrum. Methods Phys. Res. A **565**, 463 (2006); M. Abolins *et al.*, Nucl. Instrum. Methods in Phys. Res. A **584**, 75 (2008); R. Angstadt *et al.*, Nucl. Instrum. Methods in Phys. Res. A **622**, 298 (2010).
[18] M.L. Mangano *et al.*, J. High Energy Phys. **07**, 1 (2003); we use version 2.11.
[19] T. Sjöstrand, S. Mrenna, and P. Skands, J. High Energy Phys. **05**, 026 (2006); we use version 6.323.
[20] Z. Waş, Nucl. Phys. **B** Proc. Suppl. **98**, 96 (2001); we use version 2.5.04.
[21] R. Brun and F. Carminati, CERN Program Library Long

Writeup W5013, 1993.
[22] V.M. Abazov *et al.* (D0 Collaboration), Phys. Rev. D **71**, 072004 (2005); erratum-ibid. D **77**, 039901 (2008).
[23] The pseudorapidity is defined as $\eta = -\ln[\tan(\theta/2)]$, where θ is the polar angle with respect to the proton beam direction.
[24] W. Fisher, FERMILAB-TM-2386-E (2006).
[25] T. Andeen *et al.*, FERMILAB-TM-2365 (2007).